EasyChair Preprint

№ 1767

Global Path for Covering Tasks Performed by Swarming Chloroplastic Robots

Satoshi Hoshino and Shota Tezuka

EasyChair preprints are intended for rapid dissemination of research results and are integrated with the rest of EasyChair.

October 24, 2019

Global Path for Covering Tasks Performed by Swarming Chloroplastic Robots

Satoshi Hoshino[1†] and Shota Tezuka[1]

[1]Department of Mechanical and Intelligent Engineering, Utsunomiya University, Tochigi, Japan
(Tel: +81-28-689-6053; E-mail: hosino@cc.utsunomiya-u.ac.jp)

Abstract: Our chloroplastic robots are able to passively move toward a light source in a reactive manner. In this paper, we apply the swarm robotic system to a task that requires the chloroplastic robots to cover the entire environment including shadow areas. In order for the robots to achieve the covering task, we propose a global path of the light source. The light source moving along the path illuminates shadow areas. Thus the robots are able to cover the entire environment. The global path is generated in consideration of the formation of robots performing the task. Through simulation experiments, the proposed path is compared to others generated for the traveling salesman problem, TSP, and evaluated in terms of the task efficiency and performance. Finally, we discuss the effectiveness of the global path for the covering task.

Keywords: Swarm robotic systems, reactive behavior, path generation, covering task.

1. INTRODUCTION

Area covering is an important task. The task is applicable to mowing, snow shoveling, sweeping, etc. For the covering task, we use multiple mobile robots. In the field of swarm robotics, emerging behaviors from the local interaction among robots have been presented [1]. The authors have proposed a swarm robotic system inspired by the collective behavior of organelles, namely, chloroplasts [2]. Chloroplasts in plant cells move toward a light source while escaping shadows in a reactive manner. This property is called phototaxis. Consequently, the behavior similar to the chloroplasts has emerged in the swarm robotic system, as shown in Fig. 1.

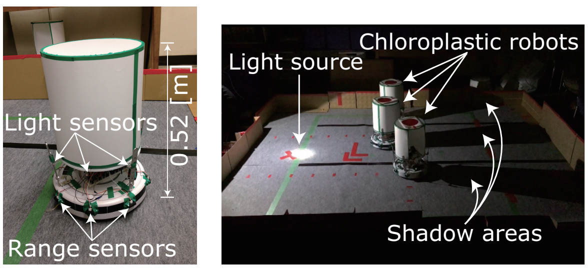

(a)Chloroplastic robot (b)Collective behavior of robots

Fig. 1 Swarm robotic system

Fig. 1(a) shows the prototype of the actual chloroplastic robot. The robot has eight range and light sensors, respectively. By using the light sensors, the robots are able to move toward a light source while escaping shadows. The range sensor allows the robot to detour around the obstacle for the collision avoidance. In Fig. 1(b), three chloroplastic robots are sweeping the environment from the right side toward the left light source.

The robots successfully swept a part of the environment without obstacles. The swarm robotic system, however, still suffers from environments with obstacles and a fixed light source as shown in Fig. 2.

Fig. 2(a) shows a simulation environment. In this environment, eight robots are vertically arranged to the light source. Since the light source is fixed at a destination in the environment, the shadow areas due to the obstacles are also fixed. In this case, the robots are able to cover the illuminated white area and pass the narrow area between the obstacles as can be seen in Fig. 2(b). On the other hand, the shadow areas remain uncovered. Furthermore, the initial formation suitable for the covering task is misaligned after the robots passed the narrow area.

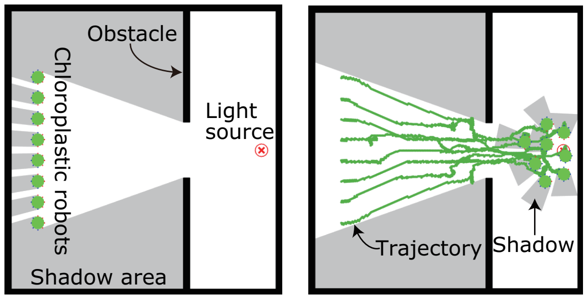

(a)Fixed light source (b)Misaligned formation

Fig. 2 Top view of simulation environment

In order for the robots to keep the initial formation, we have proposed a movement model of the light source [3]. In this paper, therefore, we propose a global path of the light source. The light source moving along the path illuminates shadow areas. Thus the robots are able to cover the entire environment including shadow areas. Through simulation experiments, the proposed path is compared and evaluated in terms of the task efficiency and performance. Finally, we discuss the effectiveness of the global path for the covering task.

2. APPROACH FOR GLOBAL PATH

In stead of a destination, subgoals are arranged all over the environment. We then generate a global path that passes through the subgoals. Graph theory based methods are one of approaches to generate such global paths. In these methods, subgoal nodes are arranged in an environment. The nodes are connected by edges. Finally, a set of edges is the generated path. In terms of efficiency, it is necessary to minimize the path length. This bench-

† Satoshi Hoshino is the presenter of this paper.

mark has been treated as the traveling salesman problem, TSP, in the field of optimization.

For the TSP, a large number of exact algorithms and heuristics have been proposed. As the number of nodes is increased to more than 20, however, it is difficult to compute the optimal (i.e. minimum) path. In this case, heuristic algorithms are used to compute a suboptimal path in a reasonable time. Especially, λ-opt [4] is a simple but effective algorithm for solving the TSP. Furthermore, meta-heuristics such as genetic algorithm, GA, and ant colony optimization, ACO [5], have been proposed.

While the TSP solvers minimize the path length, performance of multiple robots for the covering task is not taken into account. In contrast to the TSP solvers, the proposed global path is generated in consideration of the formation of robots performing the task. A light source moves along the path and visits all the nodes sequentially. Following the light source, the robots also move along the path while keeping the formation. This reactive behavior enables the robots to cover the entire environment.

3. GLOBAL PATH FOR COVERING TASK

The global path is generated through the following six steps:

1. rectangle division;
2. segmentation;
3. random node arrangement;
4. segmented paths;
5. candidate path(s); and
6. evaluation.

In the second step, the formation of robots performing the covering task is taken into account for generating the global path. In the fifth step, several candidate paths might be generated in the environment. In the sixth step, therefore, these paths are evaluated to determine the global path. Fig. 3 illustrates an example procedure.

Fig. 3(a) is a target environment. A black obstacle is located in the square. Fig. 3(b) is a result of the first step. White area in the environment is divided into two rectangles. Fig. 3(c) is a result of the second step. The rectangles in Fig. 3(b) are further segmented on the basis of the width of formation of robots, W_R. Fig. 3(d) is a result of the third step. Nodes are randomly arranged in the white area. In the fourth step, nodes in each segment are sequentially connected by edges from the one closest to a short side toward the opposite side. As a result, a local path is generated in each segment. In Fig. 3(e), these are segmented paths. Red nodes in each segmented path are defined as end nodes.

In Fig. 3(f), one of candidate paths is drawn. First off, one of two end nodes of a segmented path in Fig. 3(e) is selected as a start. After that, the other node is connected to the nearest end node of another segmented path as shown by a dashed edge. This connection process continues until all the segmented paths are connected. The other end node of the last segmented path is a goal. Since the fifth step is repeated according to the number of end nodes, the number of candidate paths corresponds to the number of end nodes. In the sixth step, these candidate paths are evaluated on the basis of the total length. Finally, the shortest one is determined as the global path.

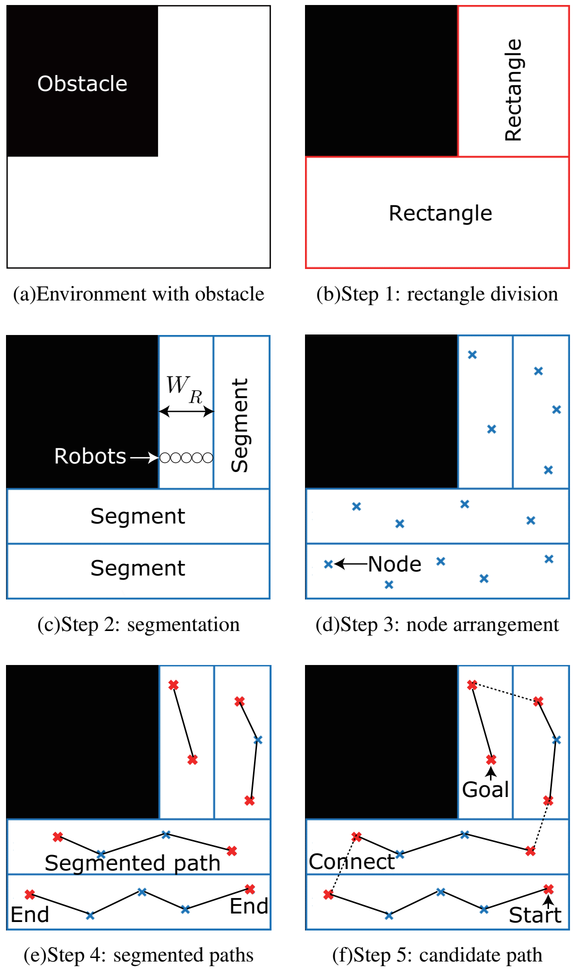

(a)Environment with obstacle (b)Step 1: rectangle division (c)Step 2: segmentation (d)Step 3: node arrangement (e)Step 4: segmented paths (f)Step 5: candidate path

Fig. 3 Procedure for generating global path (top view)

4. SIMULATION EXPERIMENT

4.1. Simulation settings

In this experiment, four chloroplastic robots are used. Each robot has a diameter of 0.3m. Thus the width of the robots' formation, W_R, is 1.2m. The maximum velocities are 0.2m/s (light source) and 0.1m/s (robots). The movement model [3] is applied to the light source. Thus the velocity vector is $\boldsymbol{v} = [v_h, v_v]$, where v_h and v_v represent the horizontal and vertical components of velocity to a current subgoal node. These are calculated from Eqs (1) and (2) as follows:

$$v_h = \begin{cases} k_1 e^{\frac{\sigma^2 - k_2}{c}} & (\sigma^2 \leq k_3) \\ k_1 e^{\frac{k_3 - k_2}{c}} & (\sigma^2 > k_3) \end{cases}, \tag{1}$$

$$\begin{aligned} v_v = {} & k_4 \left(\frac{c}{\sigma^2}\right) k_5 \omega \cos k_5 \omega t + \\ & k_6 \left(\frac{c}{\sigma^2}\right) k_7 \omega \cos k_7 \omega t + k_8 \left(\frac{c}{\sigma^2}\right) k_9 \omega \cos k_9 \omega t, \end{aligned} \tag{2}$$

where σ^2 represents the variance of robots in the vertical direction to the subgoal node. c is a constant, ω is an angular velocity, and t is a unit time. k_1 to k_9 are parameters optimized using the real-coded genetic algorithm [6].

Fig. 4 illustrates three target environments for the covering task. Each environment is surrounded by a square wall of 6×6m^2.

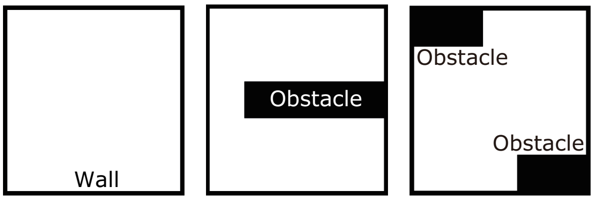

(a)Environment 1 (b)Environment 2 (c)Environment 3

Fig. 4 Top view of target environments

In environment 1, there is no obstacle (see Fig. 4(a)). In environment 2, one obstacle of 1.2×4.8m^2 is located around the center (see Fig. 4(b)). In environment 3, two obstacles of 1.2×3.0m^2 are located around the corner (see Fig. 4(c)).

In addition to the proposed global path, two other global paths are generated by using heuristic and metaheuristic algorithms, λ-opt and ACO, where $\lambda = 2$ and the number of ants is 200. Nodes are arranged in the same way in each environment. The number of nodes is 100 in environment 1, 84 in environment 2, and 76 in environment 3, to maintain the equal node density.

The covering task is finished when all the robots are within a radius of 0.9m from the goal node. These global paths are compared on the basis of the following coverage rate, C:

$$C = \frac{A_c}{A_t} \times 100, \tag{3}$$

where A_c represents the total area covered by the robots. Even if a robot covers an area already covered by another robot, the covered area is not counted. A_t represents the area colored by white in Fig. 4. Therefore, higher value of C increases the performance for the covering task.

Moreover, the following work rate, W, is used to compare the global paths:

$$W = \frac{C}{t}, \tag{4}$$

where C represents the coverage rate calculated in Eq. (3). t represents the work time of robots. Therefore, higher value of W increases the efficiency.

4.2. Simulation results

In Fig. 5, the three global paths of the light source are generated. In each result, marks "S" and "G" represent the start and goal nodes.

Although the same number of nodes was arranged at the same positions in each environment, different global paths were generated depending on the methods. In addition, the start and goal nodes were also different. Compared to the proposed path and 2-opt path, the ACO path crossed in many places. Thus the ACO resulted in the longest paths as listed in Table 1.

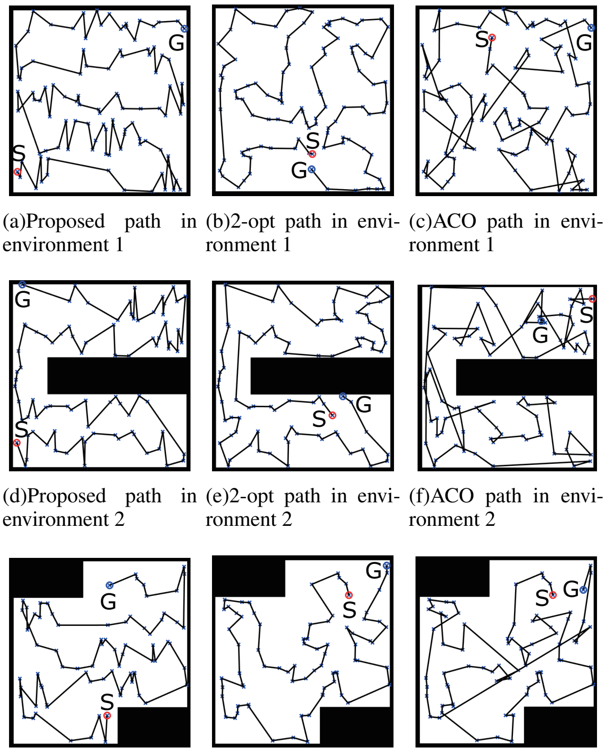

(a)Proposed path in environment 1 (b)2-opt path in environment 1 (c)ACO path in environment 1

(d)Proposed path in environment 2 (e)2-opt path in environment 2 (f)ACO path in environment 2

(g)Proposed path in environment 3 (h)2-opt path in environment 3 (i)ACO path in environment 3

Fig. 5 Generated global paths

Table 1 Comparison of total path length (m)

	Environment		
	1	2	3
Proposed path	62.9	48.6	43.9
2-opt path	44.7	43.0	34.7
ACO path	66.2	68.1	49.2

2-opt generated the shortest paths in all the environments. This result indicates that 2-opt is the most effective method for the TSP. While the proposed paths were longer than the 2-opt path, these were shorter than the ACO paths. ACO is a metaheuristic algorithm for the TSP, i.e., minimizing the path. Therefore, even though the proposed paths were generated focusing mainly on the covering task rather than the optimization, these paths were practical solutions for the TSP. In consequence, the work time spent on the covering task was increased in proportion to the path length as listed in Table 2.

Table 2 Comparison of work time (s)

	Environment		
	1	2	3
Proposed path	401	371	308
2-opt path	344	377	260
ACO path	455	553	573

Both the proposed and 2-opt paths resulted in the shorter work time than the ACO path. As for the result in environment 2, it is noticeable that, although the length of proposed path was longer than the 2-opt path as listed in Table 1, the work time of robots based on the proposed path was slightly shorter than the 2-opt path.

Fig. 6 shows the result of covering task. The area covered by the robots is painted in green. The trajectory of the light source is indicated by the red dashed line.

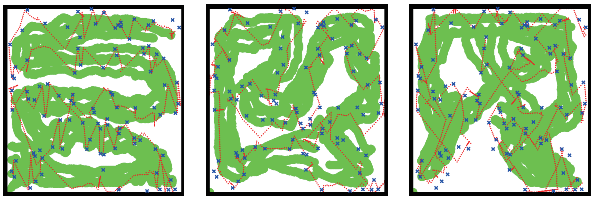

(a)Proposed method in environment 1 (b)2-opt in environment 1 (c)ACO in environment 1

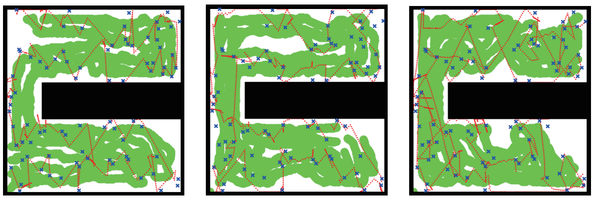

(d)Proposed method in environment 2 (e)2-opt in environment 2 (f)ACO in environment 2

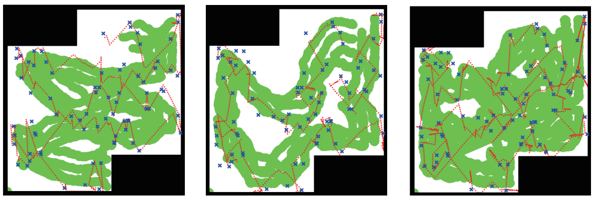

(g)Proposed method in environment 3 (h)2-opt in environment 3 (i)ACO in environment 3

Fig. 6 Covered areas and trajectories

Since the generated paths were different depending on the methods as shown in Fig. 5, the robots covered different areas. From these results, the coverage rate C and work rate W are calculated by Eqs. (3) and (4). Through the result shown in Fig. 7, we evaluate the generated global paths. The coverage rate is indicated by the bar graph and the work rate is indicated by the square plot.

Compared to 2-opt, the proposed method resulted in the better coverage rate in every environment. In environment 3, ACO resulted in the best coverage rate, whereas the work rate was the lowest. As can be seen in Figs. 6(g) to 6(i), compared to the covered area based on ACO, the proposed method and 2-opt resulted in larger uncovered areas. In this regard, however, the covered area was frequently overlapped; eventually, the ACO resulted in the lowest efficiency not only in environment 3 but also in the other environments, 1 and 2.

From the comparison and evaluation results described above, the proposed path has

- higher efficiency than the ACO path and
- higher performance than the 2-opt path.

Therefore, the proposed path is most effective for the covering task.

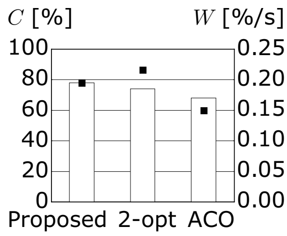

(a)Environment 1

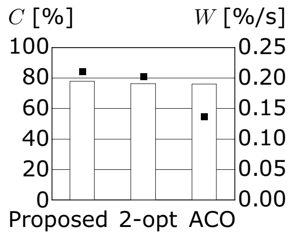

(b)Environment 2

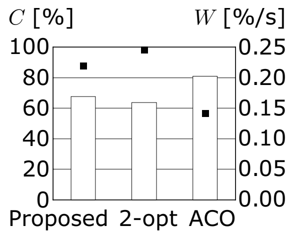

(c)Environment 3

Fig. 7 Coverage rate and work rate

5. CONCLUSIONS

In order for chloroplastic robots to cover the entire environment including shadow areas, we proposed a global path of a moving light source. The global path was generated in consideration of the formation of robots performing the covering task. Through simulation experiments, the proposed path was compared to other paths generated by using 2-opt and ACO for the TSP, and evaluated in terms of the task efficiency and performance. Finally, the effectiveness of the global path for the covering task performed by the chloroplastic robots was shown. In future works, we will generate the global path in the actual swarm robotic system as shown in Fig. 1.

REFERENCES

[1] E. Sahin, "Swarm Robotics: From Sources of Inspiration to Domains of Application," *International Workshop on Swarm Robotics*, pp. 10–20, 2005.

[2] S. Hoshino *et al.*, "Swarm Robotic Systems based on Collective Behavior of Chloroplasts," *Journal of Robotics and Mechatronics*, vol. 29, no. 3, pp. 602–612, 2017.

[3] S. Tezuka *et al.*, "External Formation Control of Swarming Chloroplastic Robots," JSME Conference on Robotics and Mechatronics, pp.1, A1–F11, 2017 (in Japanese).

[4] O. Mersmann *et al.*, "Local Search and the Traveling Salesman Problem: A Feature-Based Characterization of Problem Hardness." *Learning and Intelligent Optimization*, vol. 7219, pp. 115–129, 2012.

[5] M. Dorigo and L. M. Gambardella, "Ant Algorithms for Discrete Optimization," *Artificial Life*, vol.5, no. 2, pp.137–172, 1999.

[6] L. J. Eshleman and J. D. Schaffer, "Real-Coded Genetic Algorithms and Interval-Schemata," *Foundations of Genetic Algorithms*, vol. 2, pp. 187–202, 1993.